# A Study of the Miscibility of Polycarbonate and Poly(α-methylstyrene-co-acrylonitrile)†

**R. Silvestri,‡ M. Rink,* and A. Pavan**

*Dipartimento di Chimica Industriale e Ingegneria Chimica "G. Natta", Politecnico di Milano, P.za L. Da Vinci, 32, I20133 Milano, Italy.* *Received April 1, 1988; Revised Manuscript Received August 5, 1988*

ABSTRACT: In this paper we report on five phase diagrams of blends of bisphenol A polycarbonate (PC) and poly(α-methylstyrene-co-acrylonitrile) (αSAN) with varying molecular weight and polydispersity of αSAN. Temperature–composition phase diagram covering the temperature range from 125 °C to 180 °C were determined by examining the phase behavior—either phase separation or persistence of a single phase—of compositions purposely prepared as intimate mixtures, at any temperature. Intimate mixing of the constituent polymers was achieved by dissolution in a common solvent from which the polymer mixture was recovered via freeze-drying. Homogeneous mixtures were obtained in all cases, as revealed by a single $T_g$ intermediate between the $T_g$'s of the two pure components. The dependence of the $T_g$'s of these mixtures on their composition was subsequently used as a calibration curve for phase composition analysis. The phase behavior of each composition was determined by annealing portions of the freeze-dried, homogeneous samples at any temperature in the relevant range for time periods sufficient to reach phase equilibrium. After the thermal treatment, the samples were quenched and again analyzed via DSC. The appearance of either one or two $T_g$'s was taken as evidence for one or two phases, respectively. The composition of each phase was determined from the value of its $T_g$, using the calibration curve previously determined. All phase diagrams exhibited LCST-type miscibility gaps over the temperature range examined. Samples of different starting composition demixed into two phases belonging to different coexistence curves, one for each starting composition. The effect of αSAN molecular weight and polydispersity on the LCST behavior was examined. An attempt was made to calculate two of the phase diagrams following a scheme based on the Flory–Huggins theory.

## Introduction

In our laboratory, we have in the past studied the phase diagrams of blends of polycarbonate (PC) and poly(styrene-co-acrylonitrile) (SAN),[1] i.e., the components of the glassy matrix phase in PC/ABS blends. Both the binary PC/SAN and the ternary PC/ABS systems had previously been studied from different points of view.[2-7] As for the phase behavior of the PC/SAN system, we found that PC and SAN are immiscible in any composition over a wide range of temperatures. In this paper, we report a study on the miscibility of the bisphenol A polycarbonate (PC)/poly(α-methylstyrene-co-acrylonitrile) (αSAN) system. This blend is an upgraded variant of PC/SAN, since it shows a higher softening point. The aim of these studies is the acquisition of fundamental guidelines for the development of thermoplastic blends with a controlled structure. The temperature range examined in this work (125–180 °C) covers the range of practical interest for the industrial preparation of these blends via melt blending.

The dependence of the phase diagram on the molecular weight of αSAN was also investigated. To our knowledge, no study has been published in the literature regarding the phase diagram of this blend. For this work we used the dissolution of the two polymeric components, PC and αSAN, in a common solvent as a blending method, followed by freeze-drying. This procedure is rather laborious but seems more rigorous than others, such as melt-blending or casting the blend from a solvent (as is usually done for cloud point determinations), if the equilibrium phase diagram of the polymeric mixture is to be studied. Indeed, starting from an intimate (single-phase) mixture, the evolution toward a different (two-phase) situation can immediately be detected at the onset of phase separation from the appearance of two distinct $T_g$'s, and the final equilibrium state can be more readily reached.

As a common solvent for PC and αSAN suitable for the freeze-drying, we resorted to a mixture of two solvents, *N,N*-dimethylformamide (DMF) and *p*-dioxane (DIOX). With a two-solvent mixture, freeze-drying presents features markedly different from the usual ones when only one solvent is used. These features were also studied in this work.

An attempt to predict the phase diagrams following a scheme based on the Flory–Huggins theory is also presented (Appendix A).

**Table I**
**Molecular Characteristics of the Polymer Samples**

| | PC SINVET 271 | αSAN RI | RII | RIV | RV | SDC | PD |
|---|---|---|---|---|---|---|---|
| $M_n \times 10^{-3}$ | 15[a] | 19.3[b] | 29.1[b] | 91.6[b] | 158[b] | 91.6[c] | |
| $M_w \times 10^{-3}$ | 42.4[a] | | | | | | |
| $M_w/M_n$ | 2.83[a] | 1.2[d] | 1.2[d] | 1.2[d] | 1.2[d] | | 3.0[d] |
| $M_v \times 10^{-3}$ | 37.3[e] | 20.7[f] | 29.1[f] | 100[f] | 150[f] | | 184[f] |

[a] GPC determinations. [b] Membrane osmometry. [c] Predetermined average value obtained with a bimodal distribution (see text). [d] Estimated values. [e] Calculated from intrinsic viscosity in THF at 25 °C via the relationship $[\eta] = 3.99 \times 10^{-4}M^{0.7}$.[8] [f] Calculated from intrinsic viscosity in MEK at 30 °C via the relationship $[\eta] = 2.76 \times 10^{-4}M^{0.67}$.[9]

## Experimental Section

**Polymers.** The molecular characteristics of the samples used are shown in Table I. A single PC sample of commercial origin was used: SINVET 271 manufactured by ANIC SpA (now Enichem Tecnoresine SpA), San Donato Milanese, Italy, while the samples of αSAN were obtained from a parent random copolymer (sample PD) with azeotropic monomer composition (α-methylstyrene/acrylonitrile = 68/32 by weight) prepared by bulk polymerization. Samples RI, RII, RIV, and RV are fractions of sample PD, while sample SDC is a mixture of the fractions RII and RV in proportions such as to obtain a number-average molecular weight, $M_n$, identical with that of the fraction RIV, according to the simple rule of mixtures:

$$nM_n(\text{RII}) + (1 - n)M_n(\text{RV}) = M_n(\text{RIV})$$

in which $n$ is the mole fraction of αSAN RII.

With these samples the following systems were prepared: I, PC/αSAN RI; II, PC/αSAN RII; III, PC/αSAN RIV; IV, PC/αSAN SDC; V, PC/αSAN PD.

† Presented in part at the 16th Europhysics Conference on Macromolecular Physics, "Polymer Alloys: Structure and Properties"; Brugge, Belgium, June 4–7, 1984.

‡ Present address: Istituto Guido Donegani, I28100 Novara, Italy.

0024-9297/89/2222-1402$01.50/0 

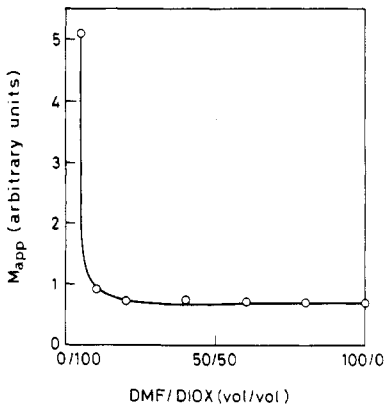


**Figure 1.** Light scattering of 5% (wt/vol) solution of αSAN PD in DMF/DIOX mixtures of varying composition. Ordinates: apparent molecular weight. Abscissae: solvent composition (see Appendix B).

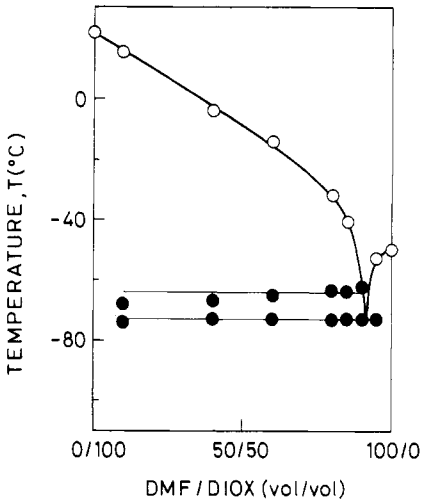


**Figure 2.** Solid–liquid phase diagram of DIOX/DMF mixtures at atmospheric pressure: (○) liquidus temperatures; (●) congruent and incongruent melting temperatures.

**Solvents.** All solvents used were reagent grade: no further purification was done.

**Measurements.** Light-scattering measurements were performed by means of a SOFICA 42000 photogoniodiffusometer, with standard measuring cells, immersed in dedusted benzene, as the transmitting liquid, in the thermostating vat. All measurements were carried out at 25 °C under unpolarized, monochromatic light (λ = 546 nm), at a scattering angle of 90°. With the aim in mind of characterizing the solubility of αSAN in solvent mixtures of various compositions, at a given polymer concentration, an "apparent" value of the solute molecular weight was determined as described in Appendix B. Differential scanning calorimetry was performed with a Mettler TA 3000 system equipped with a DSC-30 low-temperature module. Solvent mixtures were analyzed at a heating rate of 5 °C/min from −150 °C up to 30 °C; some of these scans were repeated at a heating rate of 1 °C/min. All polymeric samples were analyzed at a heating rate of 20 °C/min from ambient temperature up to 200 °C. The glass transition temperature, $T_g$, was taken as the intersection of the calorimetric trace with the median of the base lines before and after transition.

Densities were measured by means of a volume-calibrated pycnometer in a thermostated room at 25 °C.

**Freeze-Drying: Choice of Solvent.** For the freeze-drying technique the choice of the solvent is of critical importance. Several solvents common to PC and αSAN were tried in this work, but none was found to possess the characteristics (high melting point, good volatility) suitable for the freeze-drying technique, so that it was necessary to resort to a mixture of two solvents. A mixture of DIOX and DMF was thought of as suitable. In fact, DMF is by itself a solvent of both PC and αSAN (at room temperature), but it is unpractical to use in freeze-drying, due to its low melting point (−61 °C). DIOX conversely has a conveniently high melting point (12 °C) and is a good solvent for polycarbonate at room temperature, but not for αSAN. An analysis of the solubility of αSAN PD at a 5% concentration (wt/vol) in solvent mixtures DIOX/DMF of different composition was performed by light scattering at 25 °C as described in Appendix B. The results are given in Figure 1. It is evident that αSAN is soluble in solvent mixtures with 10% (vol/vol) DMF or more. Since PC is soluble in both solvents, we assumed that this composition range of the solvent mixture was also suitable for the polymer blends at the same overall polymer concentration. This assumption was supported by observation of optical transparency.

To test the suitability of these solvent mixtures under freeze-drying conditions, their melting behavior at some compositions was determined via DSC; the phase diagram (at atmospheric pressure) that can be inferred from this analysis is given in Figure 2. This diagram is typical of two components that are completely miscible in the liquid state and immiscible in the solid state,[10] with the presence of a eutectic point at −73 °C.

Assuming that these findings still hold under the working conditions (reduced pressure) applied during the freeze-drying operation, the solvent system would then consist of three phases (two condensed plus the vapor phase). Under equilibrium conditions, the phase rule holds and the system would be monovariant: once the temperature is set, the composition of the vapor, and thus its partial pressures, has to remain constant. In order to know the composition of the vapor which is obtained under the working conditions applied during the freeze-drying operation, a preliminary sublimation (in the absence of polymer solute) was performed on DIOX/DMF mixtures of 90/10, 85/15, and 80/20 (vol/vol) composition, at −30 °C. A few successive fractions of vapor were collected in the course of the process, and their composition determined via DSC measurements and the use of the diagram in Figure 2. The analysis revealed that the vapor initially collected has a composition DIOX/DMF close to 90/10, no matter what the system composition in the condensed state is.

Under the applied working conditions, it was not advisable to use a solvent mixture with a DMF content exceeding 10%; if the solvent contained a higher quantity of DMF, the condensed phase would become richer and richer in DMF, and its melting point would eventually drop below the set temperature. In conclusion, a solvent mixture DIOX/DMF with a 90/10 composition was used to perform all the freeze-drying on which we report in this paper.

**Freeze-Drying: Blend Preparation.** The αSAN samples were blended with PC in ratios of 0/100, 30/70, 50/50, 70/30, and 100/0 (by weight), according to the following procedure: 2.5 g of polymer or polymer admixtures were dissolved in 50 mL of solvent mixture DIOX/DMF 90/10; the solutions were dripped slowly into liquid nitrogen, to give rapid freezing; the spherical droplets so obtained were freeze-dried under vacuum. To speed up the removal of the last percentages of the solvent, the temperature was raised in several steps, while keeping the vacuum pump setting constant (initial vacuum = $10^{-6}$ Torr approximately). About 90% of the vapor was collected in 50 h at −30 °C; the remaining was collected while raising the temperature gradually up to room temperature. The appearance of the dried polymer blends obtained ranged from porous, low-bulk density spheres (1–5 mm in diameter) to the fine powder (particle size less than 0.1 mm) obtained for some samples of system I. All blends were washed with methyl alcohol to remove the last traces of solvent, dried in a vacuum oven at 70 °C for about 20 h, and then compacted under mild pressure to undergo DSC characterization and thermal treatment.

**Thermal Treatments.** After freeze-drying, portions of each blend were sealed in the DSC aluminum pans, then subjected to thermal treatment at different constant temperatures in the 125–180 °C range (treatments at temperatures higher than 180 °C degraded αSAN and were disregarded) for periods of time sufficient to reach phase equilibrium, and then quenched to room temperature. To assess whether phase equilibrium was reached, DSC thermograms were recorded at regular intervals, and the treatment was continued until the thermograms showed no further change. The duration of the treatments was 64 h for temperatures below 145 °C, 8 h at 155 °C, and 1 h above this temperature.

The thermal stability of the polymers may be of some concern. To check this point we performed a thermogravimentric analysis

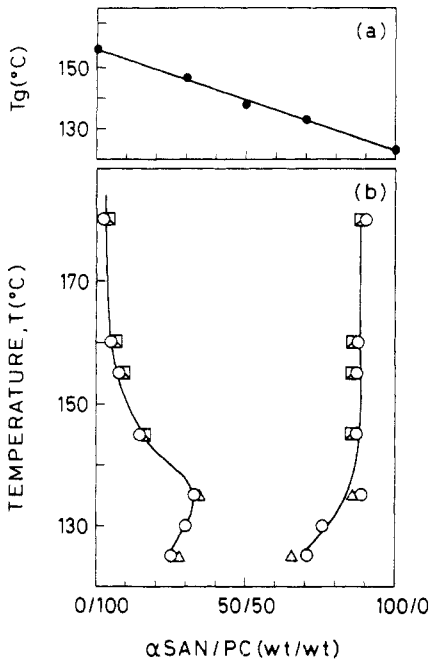


**Figure 3.** System I ($\alpha$SAN RI/PC). (a) $T_g$ of freeze-dried mixtures vs composition (calibration curve). (b) Phase diagram: (□) coexistence curve of the 70/30 PC/$\alpha$SAN mixture; (△) coexistence curve of the 50/50 PC/$\alpha$SAN mixture; (○) coexistence curve of the 30/70 PC/$\alpha$SAN mixture.

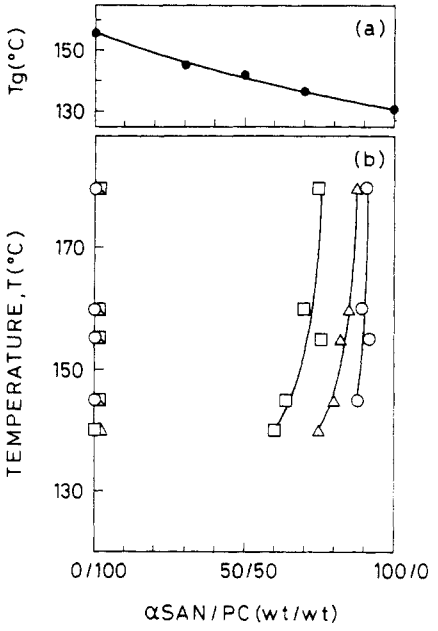


**Figure 4.** System II ($\alpha$SAN RII/PC). (a) $T_g$ of freeze-dried mixtures vs composition (calibration curve). (b) Phase diagram: symbols as in Figure 3.

on pure $\alpha$SAN PD at 180 °C under air flow. From this analysis the weight loss after 1 h is less than 1.3%. Moreover, the viscosity-average molecular weight of the same sample did not change significantly after a thermal treatment of 1 h at 180 °C under inert atmosphere.

## Results

**$T_g$–Composition Relationship.** DSC measurements on the freeze-dried preparations showed that homogeneous mixtures were obtained in all cases; each mixture exhibited a single $T_g$ intermediate between the $T_g$'s of the two pure components. The dependence of the $T_g$'s of these homogeneous mixtures on their composition is shown in Figures 3a–7a for systems I–V. Each of these curves was subsequently used as a calibration for phase–composition

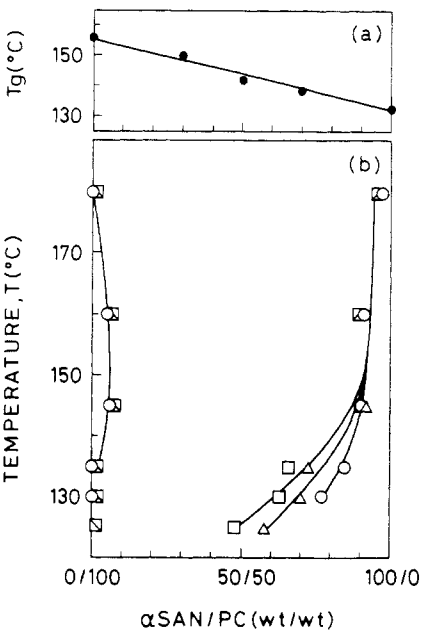


**Figure 5.** System III ($\alpha$SAN RIV/PC). (a) $T_g$ of freeze-dried mixtures vs composition (calibration curve). (b) Phase diagram: symbols as in Figure 3.

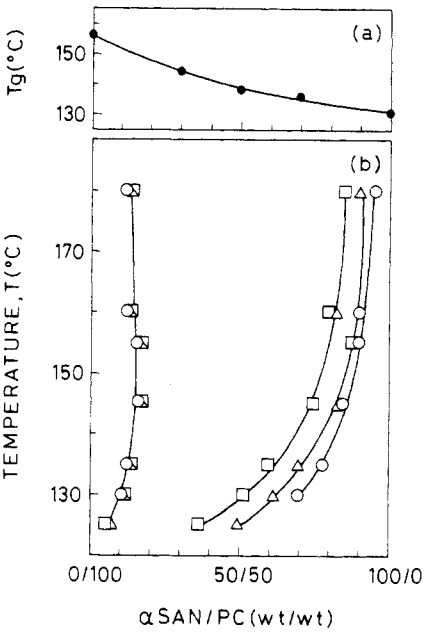


**Figure 6.** System IV ($\alpha$SAN SDC/PC). (a) $T_g$ of freeze-dried mixtures vs composition (calibration curve). (b) Phase diagram: symbols as in Figure 3.

analysis. After the thermal treatments, each blend either separated into two phases or not, depending on blend composition and temperature. The appearance of either one or two $T_g$'s was used as a criterion for regarding a blend as either one- or two-phased. When separation occurred, the composition of each single phase was determined from the value of the respective $T_g$ measured by DSC. $T_g$ values were reproducible to ±1 °C. Since the pure component $T_g$'s are 30 °C apart, the composition could be determined with an accuracy of ±5%.

**Phase Diagrams.** The phase diagrams obtained for systems I–V are given in Figures 3b–7b. Since one or both polymers were polydisperse, polymer mixtures of different composition demixed in the miscibility gap into two phases belonging to different coexistence curves, one for each starting composition, as expected.[11] The coexistence curves in question lie outside the figure plane, which is assumed

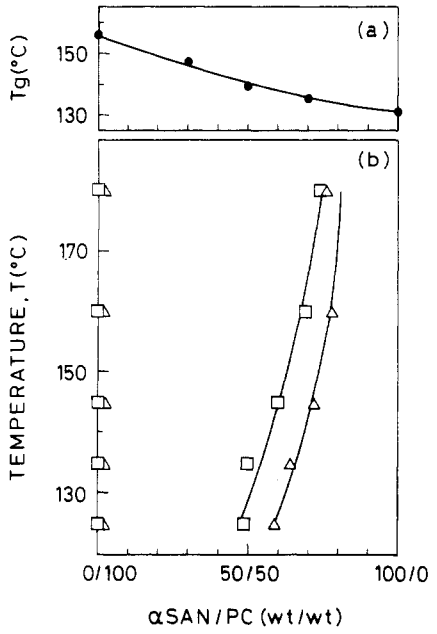


**Figure 7.** System V (αSAN PD/PC). (a) $T_g$ of freeze-dried mixtures vs composition (calibration curve). (b) Phase diagram: symbols as in Figure 3.

to be coincident with the cloud point curve plane, and can be projected onto this plane, and these projections are the ones shown in these figures. The coexistence curves displayed are those originating from the demixing of αSAN/PC mixtures of an overall composition of 30/70, 50/50, and 70/30 for systems I, II, III, and IV (Figures 3–6) and 30/70 and 50/50 for system V (Figure 7) for which the starting mixture of composition 70/30 did not show evidence of demixing at any temperature. In system II, no evidence of demixing was observed for any polymer blend examined for temperatures below 135 °C.

It should be noted that the coexistence curves are not generally closed.[12] The lowest portion of these curves would be difficult to determine in systems I, III, IV, and V, in any case, because it is situated in a temperature region in which the mobility of both macromolecular components is greatly reduced.

The effect of polydispersity of the components can be considered by comparing system III (Figure 5) and system IV (Figure 6). The αSAN component used in system IV was in fact a mixture of the two fractions RII and RV, blended in such a ratio as to obtain the same number-average molecular weight of the αSAN sample RIV used in system III, but with a bimodal molecular weight distribution (see Experimental Section). Comparison of the two phase diagrams shows no great difference: the miscibility gap in system III is only slightly wider than that in system IV: the effect of the molcular weight distribution appears to be of second order compared with the effect of the average molecular weight.

If we consider the phase diagrams obtained as a whole, some general features emerge: (a) All are of the lower critical solution temperature (LCST) type, as is generally observed in mixtures of high molecular weight components. (b) All phase diagrams appear more or less skewed toward the pure PC end, depending on the molecular weight of αSAN. (c) With the exception of system I, the miscibility gap shifts to lower temperatures as the molecular weight of αSAN increases.

## Discussion

A few remarks on the results obtained in this work are in order.

**Table II**
**Volume Fraction of Polycarbonate at the Critical Point, Calculated[a] According to Equation 1**

| system | $(\phi_{cr})_{PC}$ | system | $(\phi_{cr})_{PC}$ |
|---|---|---|---|
| I | 0.47 | III and IV | 0.67 |
| II | 0.52 | V | 0.73 |

[a] Viscosity-average degrees of polymerization were used.

The $T_g$ values measured just after freeze-drying and used to draw the $T_g$ vs composition calibration curve pertain to samples that are in an apparently expanded state, while, after the thermal treatment subsequently given to the samples, they appear in a more compacted state. The free-volume fraction could thus not be the same in the two cases. To check this point, the $T_g$'s of the pure polymers and of the blends that remained one-phased after the thermal treatment were compared with the $T_g$'s measured on the same samples just after freeze-drying: they were found to coincide within the experimental error.

Annealing treatments were also performed at temperatures a few degrees below the $T_g$'s of the two polymeric components. Under these conditions the mobility of the macromolecules is drastically reduced but can still be sufficient for segregation of macromolecules to occur, as demonstrated by the separation into two phases observed at the lowest temperatures in Figures 3 and 5–7. Due to the reduced diffusion rates, however, it is open to question whether or not complete phase separation was reached under these conditions: nothing strange in the phase diagram trends was noticed in that temperature region, however. As for the asymmetry of the miscibility gaps, it is worth recalling that the Flory–Huggins theory, as developed by Scott,[13] predicts the molecular weight dependence of the composition of the critical point as follows:

$$(\phi_1)_{cr} = \frac{1}{1 + (x_1/x_2)^{1/2}} \quad (1)$$

in which $(\phi_1)_{cr}$ is the volume fraction of polymer 1 at the critical point and $x_1$ and $x_2$ are the degrees of polymerization of polymers 1 and 2, respectively, in terms of some reference volume;[13] the ratio $x_1/x_2$ was set equal to the ratio of the molecular weights of the two polymers, $M_1/M_2$. Application of eq 1 to our systems yields the values given in Table II. Although the theory applies to systems composed of monodisperse polymers and no critical point could be determined in the present work, these values locate the miscibility gaps in fair agreement with our experimental results.

It should be noted that the coexistence curves may become ill-defined when one branch approaches the starting mixture composition, as happens, for example, in system II at lower temperatures: in this case, the second phase, pure PC, is probably produced in a small quantity that is insufficient to give a well-defined $T_g$ in the DSC analysis. Consequently, one mixture would erroneously be considered one-phased. This consideration seems to apply to the coexistence curves obtained in the demixing of the starting composition αSAN/PC 70/30 in this system, in systems III and IV, and, perhaps, in system V too, in which the right-hand branch might run close to this composition for a broad temperature range.

System I, prepared with the αSAN sample of the lowest molecular weight, shows an unexpected expansion of the miscibility gap to lower temperatures (as compared with system II). Unusual molecular weight dependence is also reported by Goh et al.[14] for the system αSAN/PMMA: the anomalous upturn in their cloud point curves in passing from lower to higher molecular weight was attributed to

**Table III**
**Values of Polymer Properties Used for Calculations**

| | PC | ref | αSAN | ref |
|---|---|---|---|---|
| $\rho$(25 °C), g/cm$^3$ | 1.19 | producer | 1.090 | this work |
| $\alpha_g(10^{-4}$ K$^{-1})$ | 1.9 | 17 | 5 | this work |
| $\alpha_l(10^{-4}$ K$^{-1})$ | 5.8 | 17 | 8.9 | 18 |
| $\delta_{Small}$ | 9.50 | 15 | 10.06 | 15 |
| $\delta_{Hoy}$ | 10.20 | 15 | 10.10 | 15 |

nonequilibrium. This does not seem to be so in our case, however, since we took special care to ascertain that thermodynamic equilibrium was reached. A possible explanation for the behavior of system I might be found in the monomer composition of this copolymer. In fact, fraction I is an extreme in the fractionation of the parent αSAN polymer (sample PD) and might have a slightly different monomer composition due to the fractionation procedure (coacervation) used. Indeed, the chemical analysis showed an acrylonitrile content of this fraction 1% above the average, a difference that is at the very limit of measurement reliability. On the other hand, it has been found that phase diagrams are extremely sensitive to copolymer composition.[11]

It is interesting to notice that, in the phase diagram of system I at 130 °C, it was found that while the 70/30 mixture of αSAN/PC underwent phase separation into two phases of composition about 25/75 and 75/25, the 50/50 and 30/70 mixtures did not demix at all. This behavior could occur near a precipitation threshold or in a temperature range in which the miscibility gap is narrow, suggesting a phase diagram with the presence of both a UCST and an LCST or with an hourglass shape.

## Appendix A

Krause's scheme[13] based on the Flory–Huggins theory was followed in attempt to predict the phase diagrams of systems II and V. For the homopolymers, the solubility parameter $\delta$ was calculated at each temperature of interest, by using

$$\delta = \rho\sum F_i/M_0 \tag{A1}$$

in which $\rho$ is the polymer density at the relevant temperature, $\sum F_i$ is the sum of all molar attraction constants of all chemical groups in the polymer repeat unit, taken from Hoy's and Small's tabulations,[15] and $M_0$ is the polymer repeat unit molecular weight.

For the copolymer αSAn, the solubility parameter was calculated by using

$$\delta = (1 - \phi)\delta_{P\alpha S} + \phi\delta_{PAN} \tag{A2}$$

in which $\phi$ is the volume fraction of acrylonitrile (AN) units in the copolymer and $\delta_{P\alpha S}$ and $\delta_{PAN}$ are the solubility parameters calculated for the two homopolymers poly(α-methylstyrene) (PαS) and poly(acrylonitrile) (PAN) according to eq A1. As to the density of the polymers, attention was paid to the fact that the theory holds under equilibrium conditions: thus the equilibrium value of the density in the liquid state was used both above $T_g$ and (by extrapolation) below $T_g$. The densities of the polymers in the liquid state, however, had to be estimated from the data available on density at 25 °C and the thermal expansion coefficients of the glassy polymers, $\alpha_g$, and of the liquid polymers, $\alpha_l$.

As observed by other authors,[16] the predictions based on Krause's scheme turned out to be very sensitive to small variations in $\delta$; inaccuracy in determining the temperature dependence of the density may markedly affect $\delta$.

With the values of $\rho$, $\alpha$, and $\delta$ given in Table III, we were able to obtain phase diagrams in qualitative agreement with the experimental ones. By using the $\delta_{\alpha SAN}$ value of 10.06 calculated from Small's tables (which falls within the range of the experimental determinations of Siow et al.[19]) and a $\delta_{PC}$ value of 9.85, intermediate between the values calculated from Small's and from Hoy's tables,[15] we obtained the phase diagrams in Figure 8 parts a and b for systems II and V, respectively.

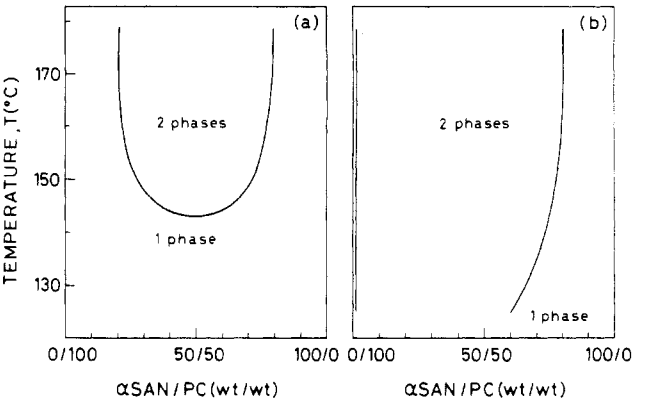


**Figure 8.** Phase diagram calculated for (a) system II and (b) system V (see Appendix A).

It has frequently been assumed in the literature (see, for example, ref 20) that the Flory–Huggins theory without proper modifications does not predict the LCST behavior commonly observed in polymer–polymer mixtures. In this work LCST behavior was predicted for the system considered, in agreement with the experimental results, by using the Flory–Huggins approach while allowing the solubility parameters $\delta$'s (affecting the Flory-Huggins interaction parameter, $\chi$) to vary with temperature, using the different thermal expaansion coefficient, $\alpha$'s, of the pure polymeric components. Other authors[16] obtained the same type of results for a similar system.

## Appendix B

Appraisal of αSAN solubility in solvent DIOX/DMF mixtures of various ratios was obtained from light-scattering measurements and the determination of an "apparent" molecular weight $M_{app}$ defined as

$$M_{app} = \frac{K\Delta i(\theta=90°,c)}{n_{solv}^2(dn/dc)^2c} \tag{B1}$$

in which $\Delta i$ is the intensity of the light scattered by the polymer, obtained as the difference between the intensities of the light scattered by the solution and by the solvent, both measured at a scattering angle $\theta = 90°$; $n_{solv}$ is the solvent refractive index; $dn/dc$ is the specific refractive index increment; $c$ is the weight/volume concentration of the solution; and $K$ is an optical constant that includes instrument calibration constants (see, e.g., ref 21, p 90).

In eq B1 the concentration and scattering angle dependence of the intensity of the scattered light, which would require double extrapolation to determine the solute molecular weight,[21] is ignored: we assume that the variation in $i$ when the polymer solubility varies with solvent composition largely overcomes virial and intraparticle interference effects.

All measurements were carried out at 25 °C with green light ($\lambda$ = 546 nm), and all optical properties are referred to these conditions. The refractive index of the solvent mixture, $n_{solv}$, was calculated from the refractive indices of the two solvents, $n_{DMF}$ and $n_{DIOX}$, assuming volume-based additivity:

$$n_{solv} = \phi n_{DMF} + (1 - \phi)n_{DIOX} \tag{B2}$$

$\phi$ being the volume fraction of DMF in the mixture.

**Table IV**
**Solvent Refractive Index and Specific Refractive Index Increment of PαS and PAN Solutions**

| polym | solv | $n_{solv}$ | ref | $dn/dc$ | ref |
|---|---|---|---|---|---|
| PαS | benzene | 1.5020 (25 °C) | 21 | 0.138 (25 °C) | 21 |
| | $CCl_4$ | 1.4596 (25 °C) | 21 | 0.168 (23 °C) | 21 |
| | cyclohexane | 1.4253 (25 °C) | 21 | 0.192 (35 °C) | 21 |
| PAN | DMF | 1.4265 (25 °C) | 22 | 0.083 (25 °C) | 21 |
| | DIOX | 1.4218 (25 °C) | 21 | | |

The specific refractive index increment, $dn/dc$, was assumed to remain constant with variations in polymer concentration and calculated by using

$$dn/dc = (n_{pol} - n_{solv})/\rho_{pol} \quad \text{(B3)}$$

in which $n_{pol}$ and $\rho_{pol}$ are the refractive index and the density of the pure amorphous polymer. For the application of eq B3 to αSAN, the density of the polymer, $\rho_{\alpha SAN}$ was measured (1.090 g/cm$^3$), while the refractive index of the polymer, $n_{\alpha SAN}$, was estimated from the data available in literature as follows.

First, mole-based additivity of the contributions of the two monomeric components was assumed according to

$$n_{\alpha SAN} = x n_{P\alpha S} + (1 - x) n_{PAN} \quad \text{(B4)}$$

in which $x$ is the mole fraction of α-methylstyrene in the copolymer and $n_{P\alpha S}$ and $n_{PAN}$ are the refractive indices of pure amorphous poly(α-methylstyrene) and poly(acrylonitrile), respectively. The value of $n_{P\alpha S}$ was estimated from a linear extrapolation of specific refractive index increment data of PαS in a few solvents against the solvent refractive index (Table IV): the intercept of that line with the $dn/dc = 0$ axis (1.699) was taken as the value of $n_{P\alpha S}$. The value of $n_{PAN}$ was obtained by reversing eq B3, applied to a solution of PAN in DMF: with the values of $dn/dc$ and $n_{DMF}$ given in Table IV and $\rho_{PAN} = 1.18$ g/cm$^3$, we obtained $n_{PAN} = 1.524$.

Finally, from eq B4 we obtained $n_{\alpha SAN} = 1.607$ and, via eq B3, the values of $dn/dc$ to be used in eq B2 could be calculated for any DIOX/DMF ratio.

**Acknowledgment.** We thank Dr. L. Kleintjens for reading the manuscript and making helpful suggestions. Financial support by C.N.R., Rome (Progetto Finalizzato Chimica Fine e Secondaria), and an A.I.R.I. Scholarship granted by E.N.I., Rome, to R.S. are gratefully acknowledged.

**Registry No.** PC (SRU), 24936-68-3; PC (copolymer), 25037-45-0; αSAN (copolymer), 25747-74-4.

## References and Notes

(1) Goisis, M. Thesis, Politecnico di Milano, 1983.
(2) Suarez, H.; Barlow, J. W.; Paul, D. R. *J. Appl. Polym. Sci.* **1984**, *29*, 3253.
(3) Riccò, T.; Rink, M.; Silicani, J.; Pavan, A. "Polymer Alloys: Structure and Properties"; 16th Europhysics Conference on Macromolecular Physics; Brugge, Belgium, June 4–7, 1984.
(4) Weber, G.; Schoeps, J. *Angew. Makromol. Chem.* **1985**, *136*, 45.
(5) Kurachi, T.; Ohta, T. *J. Mater. Sci.* **1984**, *19*, 1699.
(6) Morbitzer, L.; Kress, H. J.; Lindner, C.; Ott, K. H. *Angew. Makromol. Chem.* **1985**, *132*, 19.
(7) Locati, G., Giuliani, G. In *Rheology*; Astarita, G., Marrucci, G., Nicolais, L., Eds.; Plenum: New York, 1980; Vol. 3, p 205.
(8) Brandrup, J.; Immergut, E. H. *Polymer Handbook*; Wiley: New York, 1975.
(9) Pavan, A.; Roccasalvo, S., unpublished results.
(10) Ricci, J. E. *The Phase Rule and Heterogeneous Equilibria*; Van Nostrand: Princeton, 1951.
(11) Koningsveld, R.; Kleintjens, L. A. Contribution to the NATO Advanced Study Institute on Polymer Blends and Mixtures, London, 2–14 July 1984.
(12) Rehage, G.; Möller, D. *J. Polym. Sci., Part C* **1967**, *16*, 1787.
(13) Krause, S. In *Polymer Blends*; Paul, D. R., Newman, S., Eds.; Academic: New York, 1978; Chapter 2.
(14) Goh, S. H.; Paul, D. R.; Barlow, J. W. *Polym. Eng. Sci.* **1982**, *22*, 34.
(15) Van Krevelen, D. W. *Properties of Polymers*; Elsevier: Amsterdam, 1976.
(16) Casper, R.; Morbitzer, L. *Angew. Makromol. Chem.* **1977**, *58/59*, 1.
(17) Schnell, H. *Chemistry and Physics of Polycarbonate*; Interscience: New York, 1964; p 147.
(18) Schwarzl, F. R. In *Rheology*; Astarita, G., Marrucci, G., Nicolais, L., Eds.; Plenum: New York, 1980; Vol. I, p 243.
(19) Siow, K. S.; Goh, S. H.; Yap, K. S. *J. Chromatogr.* **1986**, *75*, 532.
(20) Paul, D. R.; Barlow, J. W. In *Polymer Compatibility and Incompatibility. Principles and Practices*; Solc, K., Ed.; MMI Symposium Series; Harwood: Chur, Switzerland, 1982; Vol. 2, p 7.
(21) Huglin, M. B. *Light Scattering from Polymer Solutions*; Academic: London, 1972.
(22) Lapcik, L.; Sundelof, L. O. *Chem. Scr.* **1972**, *2*, 41.